NETWORK SIMULATION AND SCALE–MODEL EXPERIMENTAL STUDY OF NATURAL VENTILATION IN SUBWAY STATIONS

Abstract

Thermal comfort in subway stations is usually satisfied by mechanical ventilation and an air conditioning system. However, in practice, natural ventilation exists in underground subway stations, which is driven by wind pressure, buoyancy pressure, or negative pressure caused by piston effect. It is of high significance to improve the design of an environment control system and conserve operational energy by correctly predicting the natural ventilation of the subway station with whole-sealed platform screen doors. Several subway stations in China have been tested in different seasons and different operational conditions from 2015 to 2016. The tests included the temperature, humidity, and CO_2 concentration of the outdoors and the subway stations. The distribution and the change of CO_2 concentration in the station hall floor and the platform floor were also tested and compared in the case of opening and closing the mechanical fresh air supply system. The conclusion that natural ventilation could provide adequate outdoor fresh air supply was drawn. The numerical study of the natural ventilation potential and thermal environment of a public area under different scenarios were performed by a network model-based program. The most optimized and energy-efficient operation and control strategies under different weather conditions of Shapingba subway station can be obtained based on simulations. In the end, the influence on natural ventilation, such as wind speed and direction, negative pressure caused by piston effect, and track exhaust during the train dwells, buried depth, heat load, and the number of ground entrances in a subway station were analyzed as well.

Authors

Yanan Liu, Zhen Zeng Yujie Zhang, and Yimin Xiao
Chongqing University

Keywords

Network model, natural ventilation, subway station, field measurement, numerical simulation

Introduction

In 1863, the first underground metro was constructed in London. Now the total length of subways in the world is about 6000 km (Pan et al., 2013). In the 1970s, the subway environmental simulation program (SES) (Lin et al., 2008) was developed for the simulation of airflow rates, velocity, and temperature of different subway stations. In China, STESS (Wang & Li, 2018) was developed for the simulation of the subway environment. In addition, some numerical simulation tools, such as TEST, FDS, CHMES, CFDesign, PHOENICS and CFX, were also used.

A.M. Krasyuk (2005) analyzed the piston effect when the train is in operation. The natural ventilation rates were also studied through experiments. When outdoor air temperature is below 8°C, the piston effect can meet the indoor humidity and temperature requirements without mechanical ventilation. Air movement of three new subway stations was investigated in Germany (Gerhardt & Krüger, 1998). A small-scale model experiment was conducted. The train operations and air movement determined the thermal comfort of the people in the hall layer and platform layer. Methods for controlling indoor air movement and optimizing the excessive air volume entered into stations were proposed.

The platform screen door (PSD) system has safety doors along the platform close to the track. An independent mechanical ventilation system is needed to control the environment in the tunnel of the subway stations. Because the heat exhaust system in the track will cause negative pressure in the tunnel, airflow will enter into the tunnel through screen doors when a train is stopped on the platform. This is the main reason for the leakage of air. The integration of CFD and network model simulations is the major research method to study this process. Don Willemann and J.Greg Sanchez (2002) retrofitted the fan plant to improve the security of the tunnel ventilation system in New York City. The advantages for integration of the field simulation program with the network simulation program was emphasized. D. McKinney and P. Miclea (2003) used the simulation results of the SES program as the boundary conditions for the CFD simulations. Transient simulations were conducted to calculate the air change rate when the screen door was open. But the influence of train operation in the upstream and downstream was neglected. The effect of thermal buoyancy, the obstacle of on-off passengers was neglected as well. Lin-Jye Chun et al. (2004) integrated SES with CFD. The pressure distribution on the screen door (PSD) subjected to a moving train running through a station in the tunnel was investigated. The advantages of this screen door design were analyzed.

Most of the research about the screen door system was focused on the air exchange between the screen door and the tunnel. The effect of buoyancy was neglected as well. In terms of research methods, 3D numerical simulation with SES was the most popular case. The geometrical model was complicated, it was time-consuming to build the model and proceed to simulations. Furthermore, tunnel, station, and outdoor environment was not simulated simultaneously as a whole. And the dynamic on-off process of screen door was not captured as well. In our study, small experimental studies with network model simulations were conducted. A dynamic network model considered the buoyancy effect and screen door on-off process was proposed to analyze the indoor environment of the subway station.

Network Methods

MASS FLOW BALANCE EQUATIONS OF NODES

One-dimensional multizone network model is implemented, which is based on graph theory and looped method (Liu et al., 2019). If there are *m* nodes and *n* branches in the network, the mass balance equation of the ith node is expressed as Equation 2.1:

$$\sum_{j=1}^{n} a_{ij} M_j = 0$$

where a_{ij} is a sign function. If a_{ij} = -1, it denotes that node i is the ending node of branch j; if a_{ij} = 1, it denotes that node i is the starting node of branch j; and if a_{ij} = 0, it denotes that node i is not located at branch j. M_j (j = 1 ~ *n*) represents the mass flow rate of the jth branch. Figure 1 shows the network of the underground subway station.

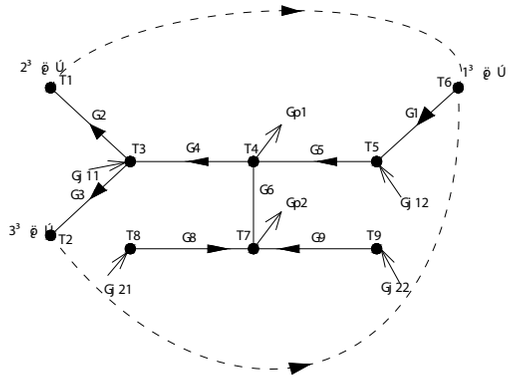

Figure 1: Network of the underground subway station.

THERMAL BALANCE OF NODES

The branch direction is first assumed to be the same as the flow direction. If the heat loss at the nodes is neglected, the heat balance equation of node *i* is written as Equation 2.2:

$$\sum_{j=1}^{n} a_{x1.ij} . C_P . |M_j| . t_{sta,j} + \sum_{j=1}^{n} a_{x2.ij} . C_P . |M_j| . t_{end,j} = 0$$

where c_p represents the air specific heat, 1.01kJ/(kg.K); represents the flow temperature at the start of the jth branch, °C; $t_{end,j}$ represents the flow temperature at the end of the jth branch,°C; and $a_{x1,ij}$ and $a_{x2,ij}$ are sign functions. If the flow of the jth branch comes from node i, $a_{x1,ij}$ = 1; otherwise, $a_{x1,ij}$ = 0. If the flow of the jth branch enters node i, $a_{x2,ij}$ = 1; otherwise, $a_{x2,ij}$ = 0.

THERMAL BALANCE OF BRANCHES

The thermal balance equation for the jth branch is written as Equation 2.3:

$$C_P |M_j| (t_{sta,j} - t_{end,j}) = Q_{f,j} - Q_{w,j}$$

Where $Q_{f,j}$ represents the convective heat release rate in the jth branch, kW; $Q_{w,j}$ represents the heat loss of the jth branch.

PRESSURE BALANCE OF FLOW LOOPS

The flow network is composed of loops. For the k^{th} loop, the total pressure rise is equal to the pressure loss resulting from flow resistance. The pressure balance equation of the flow loop is written as Equation 2.4:

$$\Delta P_{r,k} = P_{b,k}$$

where $\Delta P_{r,k}$ is the pressure loss resulting from flow resistance in the k^{th} loop; $P_{b,k}$ is the pressure change caused by the thermal buoyancy in the k^{th} loop.

The total pressure loss resulting from flow resistance in the k^{th} loop, $\Delta P_{r,k}$, is composed of the pressure loss of all branches located in the k^{th} loop (Equation 2.5):

$$\Delta P_{r,k} = \sum \Delta P_{r,j}$$

If there is a height difference between the starting point and ending point of the j^{th} branch, thermal buoyancy force is generated and is expressed as Equation 2.6:

$$P_{b,j} = \rho_0 \left(1 - \frac{T_0}{T_{f,j}}\right) . g . \Delta Z_j$$

where ΔZ_j is the height difference between the actual flow ending and starting nodes of the smoke-occupied j^{th} branch and is the spatially averaged temperature in the j^{th} branch.

Experiments Setup

To balance the realization and cost, the geometry similarity scale was C_l=1:20. Because this study is mainly focused on buoyancy natural ventilation, Archimedes numbers should be identical for prototype and model.

$$Ar = \frac{gl\Delta T_0}{(v_0)^2 T_u}$$

(Equation 3.1)

$Ar_m = Ar_n$, according to Equation 2.1,

$$\frac{g_m l_m \Delta T_{0m}}{(v_{0m})^2 T_{0m}} = \frac{g_n l_n \Delta T_{0n}}{(v_{0n})^2 T_{0n}}$$

(Equation 3.2)

Equation 2.1 could be derived to:

$$\frac{C_g . C_l . C_{\Delta T_0}}{(C_{v_0})^2 . C_{T_0}} = 1$$

(Equation 3.3)

Because we mainly consider the buoyancy ventilation, $Arq_m = Arq_n$, Equation 2.3 could be derived to:

$$\frac{g_m l_m q_m}{C_{pm}\rho_{0m}(v_{0m})^3 T_{0m} F_m} = \frac{g_n l_n q_n}{C_{pn}\rho_{0n}(v_{0n})^3 T_{0n} F_n}$$

(Equation 3.4)

Because $C_{pm} = C_{pn}$, $\frac{F_m}{F_n} = C_l^2$, Equation 2.4 could be derived to:

$$\frac{C_g . C_q}{C_{\rho_0} . (C_{v_0})^3 . C_l . C_{T_0}} = 1$$

(Equation 3.5)

The total air supply $Q = p_0 \cdot V = p_0 \cdot v_0 \cdot F$,

$$C_Q = \frac{Q_m}{Q_n} = C_{\rho_0} . C_{v_0} . C_F$$

(Equation 3.6)

Where p_0—density of supply air, Kg/m³; v_0—Mean air velocity, m/s; F— sufficient area of supply louver, m².

Parameters	Geometry similarity	Pressure	Temperature difference	Velocity	Air flow rates	Heat flux
Ratio	1/20	1	1/1	1/4.4721	1/1789	1/1789

Table 1: Summary of scale ratios.

According to ideal gas equation of state $P \cdot V = m \cdot R \cdot T$,

$$C_{\rho_0} = \frac{\rho_{0m}}{\rho_{0n}} = \frac{B_m}{B_n} = C_B$$

(Equation 3.7)

Where B_m—local atmospheric pressure of small-scaled model; B_n—local atmospheric pressure of prototype C_B—Scale ratio of atmospheric pressure.

Acceleration of gravity is constant, so gravity ratio $C_g = 1$. Keep the supply air temperature identical between prototype and model, temperature ratio $C_{T_0} = 1$. The small-scaled model and prototype are both in Chongqing, where the atmospheric pressure is 97320Pa in summer and 99120Pa in winter. Hence, the similarity ratio of atmospheric pressure is $C_B = 1$. Based on Equations 2.3, 2.5, and 2.6, we can obtain...

Velocity scale ratio:

$$C_{v_0} = (C_l)^{1/2} = 1/4.4721$$

Air flow rates scale ratio:

$$C_Q = C_B \cdot C_{v_0} \cdot C_F = C_B \cdot (C_l)^{5/2} = 1/1789$$

Space zone	Prototype			Model		
	length	width	height	length	width	height
Hall floor	80000	20000	6000	4000	1000	300
Platform floor	118000	10000	4000	5900	500	200
Corridor of entrance	50000	6000	3000	2500	300	150

Table 2: Geometrical dimensions of prototype and scale model (units: mm).

Heat flux scale ratio:

$$C_q = C_l \cdot (C_{v_0}) \cdot C_p = C_B \cdot (C_l)^{5/2} = 1/1789$$

The summary of scale ratios is indicated in Table 1.

Based on the above calculations, the dimensions of the small-scaled model are summarized in Table 2. And the small-scaled model is illustrated in Figure 3. When a train was stopped in the platform of the tunnel, most of the heat generated by air conditioning in the train was released to the tunnel near the platform. To keep the air temperature relatively stable in the tunnel, an exhaust fan was in operation. This approach resulted in negative pressure in the tunnel, and airflow inside the station traveled to the tunnel through the screen door of the platform.

To simulate this process, two exhaust fans were installed in the tunnel. When the screen door was open, the natural ventilation in the station was induced by wind pressure and thermal pressure. When the screen door was closed, the natural ventilation was induced by wind pressure, thermal pressure, and negative pressure effect of the tunnel. As indicated in Figure 3, heat effect was considered according to the similarity theory. Heat flux scale ratio was 1/1789. The carbon fiber wire was used to capture this heat unit.

For the platform floor, advertisement board, IT equipment, lighting, human beings, heat release from condenser, heat transfer from screen door, and envelope heat transfer was considered. For the hall floor, advertisement board, LED indicator, ticket and food vending machines, ticket counter, subway brake, ATM machine, security checking machine, shopping stores, lighting, human beings, and envelope heat transfer was considered. For the exit corridor, escalator, lighting, human beings, and envelope heat transfer was considered.

The arrangement of testing point is indicated as Figure 3. A Type T thermal couple was used to measure indoor air temperatures. A Testo 835-T1 infrared thermometer was used to measure the surface temperature. Multifunction measuring instrument Testo 480 was used to measure the air velocity, air temperatures, and humidity.

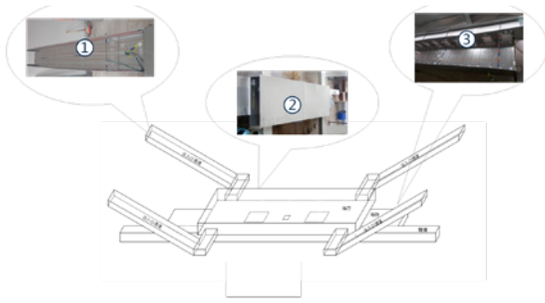

Figure 2: Scale model setups. 1) Corridor of entrance. 2) Hall floor. 3) Platform floor.

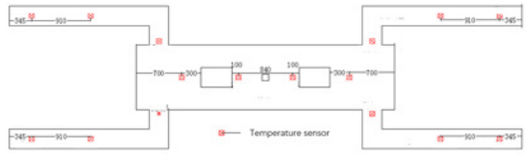

Figure 3: Temperature sensor arrangement.

Results and Discussions

To investigate how different parameters and aspects influence the thermal performance of underground subways, 12 different scenarios were arranged. As indicated in Table 3, different heat loads, number of entrances, buried depth of stations, and relative height difference of entrances were designed to investigate how these parameters affect the natural ventilations. As shown in Figure 4, there are three entrances for scenarios 1–4, two entrances for scenarios 5–6, four entrances for scenarios 7–8, and two entrances for scenarios 9–12. Scenarios 1–3 have different buried depths for stations. For scenarios 3–4, 5–6, and 7–8, they share the same number of entrances respectively, while they have different strengths of heat sources. For scenarios 9–12, they all have two entrances while they possess difference height variance between these entrances

.

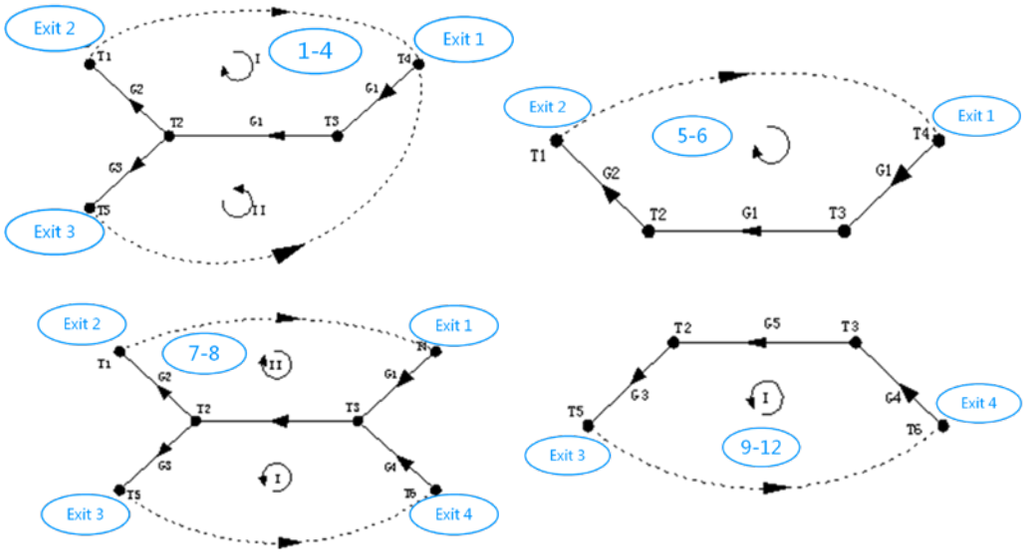

Figure 4: Network schematic of 12 scenarios.

	Heat flux (W)						Air Temp. (°C)	En. H (m)			
No.	Hall	Platform	En.1	En.2	En.3	En.4		1	2	3	4
1	530	530	0	0	0	NA	33.8	0.4	0.4	0.4	NA
2	530	530	0	0	0	NA	33.8	0.8	0.8	0.8	NA
3	530	530	0	0	0	NA	33.8	1.2	1.2	1.2	NA
4	530	530	121	118	0	NA	33.8	1.2	1.2	1.2	NA
5	530	530	0	0	NA	NA	34	1.2	1.2	NA	NA
6	530	530	121	118	NA	NA	34	1.2	1.2	NA	NA
7	530	530	0	0	0	0	34	1.2	1.2	1.2	1.2
8	530	530	61	62	62	62	36	1.2	1.2	1.2	1.2
9	522	525	0	0	NA	NA	27.5	NA	NA	1.2	1.0
10	522	525	0	0	NA	NA	27.5	NA	NA	1.2	0.8
11	522	525	0	0	NA	NA	27.5	NA	NA	1.2	0.6
12	522	525	0	0	NA	NA	27.5	NA	NA	1.2	0.4

Table 3: The working conditions of the model experiment.

Based on the comparison between simulations and experiments as shown in Figure 5, these results show good agreements. We can see from scenarios 1–3, they have different buried depths of 0.4m, 0.8m, and 1.2m in the small-scaled model (8m,16m, and 24m in the prototype). When the buried depth increases, the average temperature of the hall layer decreased significantly. For scenarios 3–4, 5–6, and 7–8, the average temperature changes when heat flux was considered in the exits. For scenarios 9–12, the height difference increased, while the average temperature shows little difference. We can know that the buried depth plays relatively critical roles comparing height difference among different exits.

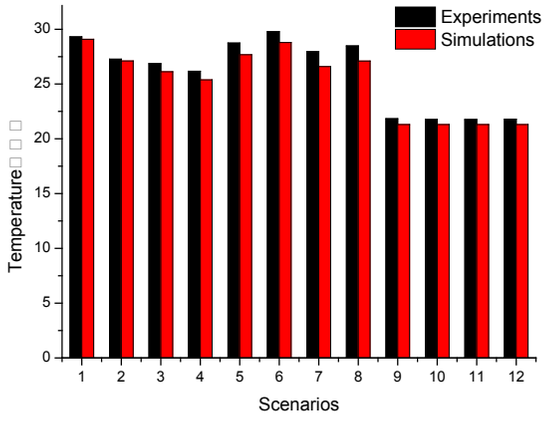

Figure 5: Average temperature comparison between experiments and simulations for 12 scenarios.

CHANGE THE BURIED DEPTH OF STATIONS

After this validation, we also conducted detailed dynamic simulations according to different buried depths (10m, 15m, 20m, 25m, and 30m). We conducted the simulations according to weather conditions of Chongqing. The outdoor temperature is 18.9°C; daily wave length is 3°C; and mechanical ventilation rates are 12m3/s. As shown in Figure 6, the average temperatures in the hall layer has no obvious differences. We can see Figure 7 has the similar results for the platform layer. But according to Figure 8, the total airflow rates increases about 4 m3/s. When the depth of the subway station increases, the thermal buoyancy pressure increases. The total airflow rates increase, which will result in decreasing of CO_2 concentrations and increasing of the fresh airflow rates. Regarding the average temperature of the subway stations, no significant changes occurred because the heat transfer from the envelope increased. Hence, the heat load increased following with the increase of the total airflow rates. As a whole, the depth of the subway stations will have significant effect on the total fresh airflow rates while having limited effect on the thermal environment inside the subway stations.

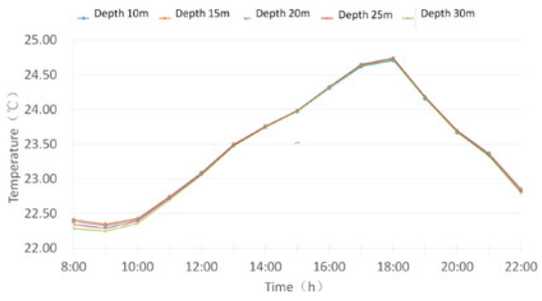

Figure 6: Average temperatures of different buried depths in the hall layer.

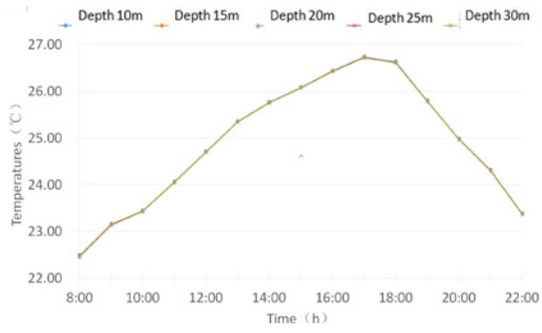

Figure 7: Average temperatures of different buried depths in the platform layer.

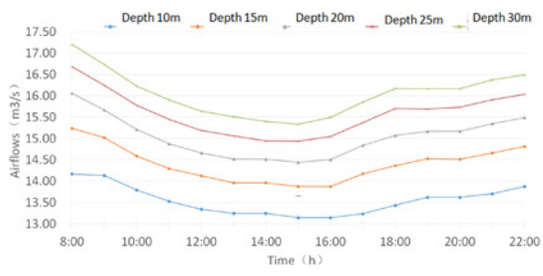

Figure 8: Hourly total airflow rates of different buried depths.

CHANGE THE NUMBER OF EXITS

According to the code for design of metros in China, the minimum number of exits is two. The number of exits will affect the flow resistance of the whole subway station. This variation will influence the ventilation performance of the whole station. We conducted the simulations according to weather conditions of Chongqing. The outdoor temperature is 18.9°C; the daily wave length is 3°C; and the mechanical ventilation rates are 12m3/s. The number of exits is two, three, and four respectively.

As shown in Figure 9, the hourly average temperature of the hall layer was obtained based on simulations. When the number of exits increases from three to four, the cooling effect enhanced significantly. The temperatures decreased approximately 2°C.

As illustrated in Figure 10, the hourly average temperature of the platform layer changes slightly when we alter the number of exits. We can know that the effect of changing the number of exits is not so obvious. As seen from Figure 11, the hourly total airflow rates increase significantly when we change the number of exits from three to four. This result shows good agreement compared with the average temperature of the hall layer. Based on these results, we can know that when the number of exits increases, the natural ventilation rates increase significantly, thereby decreasing the average temperature of subway stations. These simulations show the importance of optimizing the number of exits in terms of natural ventilation design in subway stations.

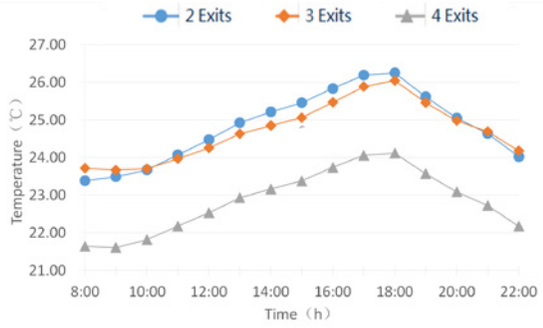

Figure 9: Hourly average temperature of the hall layer based on different exits.

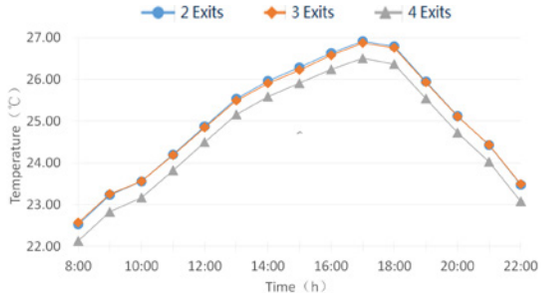

Figure 10: Hourly average temperature of the platform layer based on different exits.

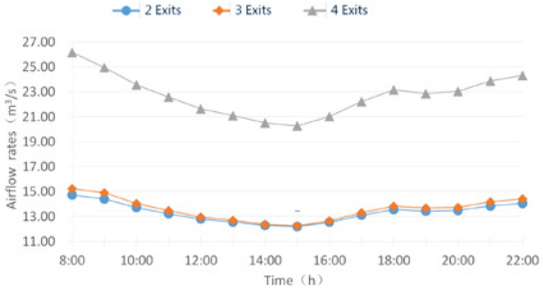

Figure 11: Hourly total airflow rates based on different exits.

Conclusions

Numerical simulations and a small-scaled experiment was conducted. Twelve different scenarios were measured and compared with numerical simulation results, which shows good agreement. Firstly, we can conclude that the network method is quite reliable for the prediction of natural ventilation and temperature distributions of the underground metro. Secondly, thermal buoyancy pressure as the main driven force is mainly affected by the internal heat source and buried depth of the station rather than the relative height difference of different entrances. Thirdly, natural ventilation induced by thermal buoyancy can effectively reduce the temperature of the corridor and station hall. Because the long flow path of the natural ventilation, the airflows enter from the entrance, then flow into the corridor and hall and finally into the platform. Due to the resistance and long distance, the temperature of the airflow increases gradually. The cooling effect for the platform is attenuated. Lastly, when the number of entrances increases and the heat source of the entrances decreases, the airflows of natural ventilation increase. This strategy will improve the thermal environment of the platform floor.

Based on the simulations and experiments, we have some suggestions for the design of underground subways. Firstly, according to the normal design of underground subways in China, the mechanical ventilation of the platform layer and hall layer account for 55% and 45% of the total amount of airflows, respectively. Based on the results of experiments, the thermal environment of the hall layer could be improved significantly due to the natural ventilation driven by thermal buoyancy and negative pressure effect. However, the platform layer is not enhanced so well. Hence, we recommend that the ratio of mechanical ventilation between platform layer and hall layer should be adjusted. The mechanical ventilation of the platform layer should be increased while the amount of mechanical ventilation of the hall layer should be reduced. Secondly, minimizing the heat source of the corridor can attenuate the heating of the airflows. Lastly, the stack ventilation concept should be introduced to the design of underground subways. By integrating the design of a solar chimney, stack, or atrium with the traditional subway stations, we can scientifically improve the performance of the underground subway stations.

Acknowledgements

The authors acknowledge the support from National Natural Science Foundation of China (NSFC) (51678088, 51578087, 51178482), and the National Key R&D Program of China under Grant No. 2016YFC0800603. Yanan Liu is also especially thankful for the scholarship provided by the China Scholarship Council (SCS student ID: 201706050003).

References

Chun, L.-J., Chiang, Y.-C., Ting, C.-C., Ma, R.-H., & Chen, S.-L. (2004). Pressure Analysis of Platform Screen Door Subjected to a Moving Train in Mass Rapid Transport Underground Station. *Journal of Mechanics*, *20*(2), 159–166.

Gerhardt, H. J., & Krüger, O. (1998). Wind and train driven air movements in train stations. *Journal of Wind Engineering and Industrial Aerodynamics*, 74–76, 589–597. doi:https://doi.org/10.1016/S0167-6105(98)00053-1

Krasyuk, A. (2005). Calculation of tunnel ventilation in shallow subways. *Journal of Mining Science*, *41*(3), 261–267.

Lin, C.-J., Chuah, Y. K., & Liu, C.-W. (2008). A study on underground tunnel ventilation for piston effects influenced by draught relief shaft in subway system. *Applied Thermal Engineering*, *28*(5), 372–379. doi:https://doi.org/10.1016/j.applthermaleng.2007.10.003

Liu, Y., Xiao, Y., Chen, J., Augenbroe, G., & Zhou, T. (2019). A network model for natural ventilation simulation in deep buried underground structures. *Building and Environment*, *153*, 288–301.

McKinney, D., & Miclea, P. (2003). Use of CFD to estimate airflow through PSDs during train dwell. Paper presented at the 11th International Symposium on Aerodynamics & Ventilation of Vehicle Tunnels. UK: BHR GROUP.

Pan, S., Fan, L., Liu, J., Xie, J., Sun, Y., Cui, N., . . . Zheng, B. (2013). A review of the piston effect in subway stations. *Advances in Mechanical Engineering*, *5*.

Wang, Y., & Li, X. (2018). STESS: Subway thermal environment simulation software. *Sustainable Cities and Society*, *38*, 98–108. doi:https://doi.org/10.1016/j.scs.2017.12.007

Willemann, D., & Sanchez, J. G. (2002). Computer modeling techniques and analysis used in design of tunnel ventilation fan plants for the New York City Subway. Paper presented at the Railroad Conference, 2002 ASME/IEEE Joint.